대한기계학회 2001년도 추계학술대회논문집 A pp. 477~482 KSME 01F079

New Milliactuator Embedded Suspension

Joon-Hyun Yoon*, Eo-Jin Hong*, Hyun Seok Yang** and Young-Pil Park**

밀리엑츄에이터가 내재된 신규 서스펜션

윤 준현· 홍 어진· 양 현석· 박 영필

Key Words: Milliactuator(밀리엑츄에이터), Servo Bandwidth(서보 대역폭), Piezoelectric(피에조), Suspension(서스펜션)

Abstract

To realize higher track density of HDD, the servo bandwidth should be higher, however, is limited by the mechanical resonances of the arm, coil of the VCM and ball bearing pivot. The dual-stage actuator systems have been suggested as a possible solution. For the dual-stage actuator systems based on the suspension, the suspension resonance frequencies in the radial access direction are important factors to increase a servo bandwidth, however the improvement of these frequencies may affect the shock resistance performance and spring constant. The slider's flying stability can be deteriorated by the change of a vertical stiffness. In this work, we have investigated a suspension design scheme possessing a milliactuator for dual-stage actuator systems and also achieved higher mechanical characteristics. Design parameters are deduced by finite element analysis with sensitivity function. It is confirmed that the proposed suspension with the milliactuator has the capability of fine tracking motion, due to its hinge structure on the spring region, and achieves higher mechanical resonance frequencies in the radial access direction with a high-shock resistance and a low-spring constant.

1. Introduction

The hard disk drive (HDD) has been the primary leader for data storage systems in storing data inexpensively. Since 1956 when IBM built the original hard disk drive, known as RAMAC, the HDD has been developed to achieve large data storage capacity for storing information on computers. The storage capacity most often quoted for HDD is the areal density, which is the product of linear bit density and radial track density. Linear bit density which is expressed bits per inch (BPI) is going to close to the upper limits of what may be technologically feasible. Maintaining the current impressive growth rate will be achieved mainly through an increase in radial track density which is expressed tracks per inch (TPI).

The servo control of track follow mode is to hold the head as close to the track center as possible for errorless reading and writing. According to the increase in track density, the servo control system for HDD should stay the head within increasingly tighter limits for reading and writing information. This limit means the offset between the actual head position and the track center, called the track misregistration (TMR), which amounts to about 10-12% of the track-to-track pitch. As a result of the decrease of the track pitch, the allowable level of TMR drops so that the allowable level of vibrations for lower TPI becomes even

* Dep. of Mech. Engineering, Yonsei Univ.

** Professor, Dep. of Mech. Engineering, Yonsei Univ.

more troublesome. The feasibility of the maximum TPI is determined by TMR, which is strongly related to open loop servo bandwidth [1]. There are several difficulties with a conventional actuator system to realize higher servo bandwidth for higher track density. To solve this problem, various types of dual-stage actuators have been suggested by many researchers [2],[4],[6],[7].

2. Microactuator and Milliactuator

2.1 Classification of Dual-Stage Actuator Systems

Dual-stage actuator systems for HDD can be classified into several types in respect to electrical-to-mechanical energy conversion schemes of the secondary actuator and also in respect to the location of the secondary actuator. According to the driving force, secondary actuator systems are classified into three groups: electrostatic, electromagnetic, and piezoelectric actuators. With respect to the secondary actuator's location, dual stage actuator systems are divided into four groups: moving magnetic head, slider, suspension and arm. The secondary actuator moving magnetic head or slider is realized using micro structures, so that is called the microactuator. The last two moving types are generally called the milliactuator.

2.2 Characteristics of Milliactuator

Placing the microactuator in the gimbal area requires that the manufacturing cost, flying characteristics, and electrical characteristics should be resolved. Despite the limitation that a large voltage may be required to attain even small displacements, the PZT milliactuator driving the suspension is expected to serve as a bridge between single-stage actuator and dual-stage actuator [5].

Based on the piezoelectric elements, piezoelectric microactuators are classified into three types; stack, planar and shear type. The shear type PZT distinguishes itself from other types of PZTs in terms of the displacement constant characteristic. Namely, the displacement per voltage of the shear type PZT is independent of the dimension of the element as shown in Eq. (1).

$$\Delta L / V = n \cdot d_{15} \qquad (1)$$

where ΔL is the displacement of the shear type PZT, V is the applied voltage, n is the number of layers, and d_{15} is the shear charge coefficient.

By virtue of the independence from dimension, the shear type PZT has an advantage to be designed small and thin [6].

In this work, the secondary actuator is milliactuator that is based on shear type PZT driving the suspension

3. Milliactuator Embedded Suspension

3.1 Suspension for Dual-Stage Actuator [7]

Pacing the milliactuator on the front of the base plate, the servo bandwidth of the dual-stage actuator is decided by the flexibility in the radial access direction of the suspension. This means that the servo bandwidth is affected by the 2nd torsion or sway mode of the suspension. If the suspension is simply modified to enhance theses resonant frequencies, the slider's flying stability can be deteriorated by the change of a vertical stiffness.

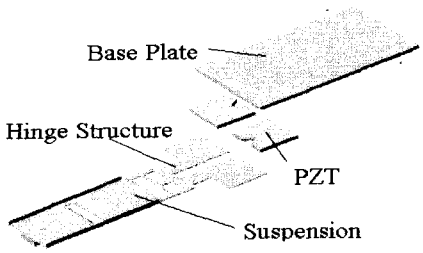

Fig.1 Schematic view of the suspension with milliactuator

In this work, the hinge structure of the milliactuator is designed on a spring region to work as a vertical spring, therefore, the additional element for the dual-stage actuator system is PZT only as shown Fig 1. Then, the remaining problem is how to design a suspension adequately to have abilities of higher servo bandwidth and the slider's flying stability.

3.2 New Suspension with Milliactuator

The suggested suspension with integrated milliactuator takes a rectangular shape that can have signal pattern layers for the GMR head and the gimbal structure like pico-CAPS [3]. The suspension has integrated signal pattern and the gimbal structure that results in minimizing handling damage and assembly tolerance in the manufacturing process and then this type suspension is called two-piece suspension which consists of a gimbal embedded load beam and a base plate. If the integrated gimbal structure is designed like the torsion bar style, the slider movement during the shock separation can be less likely to cause damage than the gimbal in conventional three-piece suspension, which is composed of the load beam, the gimbal and the base plate.

4. Finite Element Analysis

4.1 Design Variables for Suspension

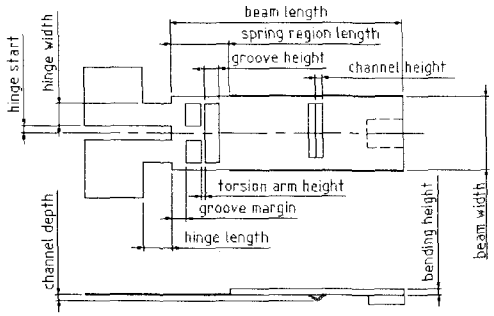

Fig.2 Definition of design variables

In the process of suspension design, design parameters are selected to be hinge shape, spring region shape, and beam shape as shown in Fig. 2.

The hinge shape means hinge position described by hinge start, hinge length, and width. The beam shape includes beam width(BW), beam length(BL), and side bending height(SB). The spring region shape is composed of spring region length(SL), groove margin(GM), height(GH), and torsion arm height.

Additional stiff elements on the nodal point at a high-strain energy location of the torsional mode, makes the torsional mode frequency high [9]. Based on this concept, the channel is designed as additional stiffer to have higher torsional mode for a higher servo bandwidth.

4.2 Finite Element Model

Finite element analyses are performed using the software ANSYS. Four node shell elements (SHELL63) are used for the suspension except the pico slider, and 8 node brick elements (SOLID45) are used for the slider. The entire model is composed of 498 elements and 605 nodes. The elements consist of 474 SHELL63 and 24 SOLID45. Table 1 shows the material properties for the model.

Table 1 Material properties used in model

Component	Young's modulus [GPa]	Density [kg/m3]	Poisson ratio
Load beam	193	8030	0.29
slider	412	4250	0.27

4.3 Sensitivity Analysis for Design Variables

Sensitivity analysis, the study of changes in system dynamic characteristics with respect to parameter variation, is conducted in a variety of engineering disciplines [10].

In this work, sensitivity function is deduced by the variation of design variables through FEM.. Design variables with respect to the hinge shape are determined by performances of the milliactuator. We intend that resonance frequencies shall be changed from the original to target values by changing design variables with sensitivity function. The original and the target values are obtained based on physical insight and observations. These resonance frequencies are related to cantilever mode for the slider flying stability, the 2nd torsion and sway mode for higher bandwidth of the milliactuator. The finite model modifying algorithm is represented as follows [11].

step1) Define the design variable vector $\underline{\zeta}$ for structural modification. There are 6 variables related with the beam shape and the spring region shape.

$$\underline{\zeta} = [\zeta_1, \zeta_2, \zeta_3, \zeta_4, \zeta_5, \zeta_6]^T \quad (2)$$

step2) Construct a frequency vector θ with three frequencies, which are related to the cantilever, the 2nd torsion, and sway mode.

$$\underline{\theta} = [\theta_1, \theta_2, \theta_3]^T \quad (3)$$

Define the target frequency vector $\underline{\theta}_T$ and the current frequency vector $\underline{\theta}_C$ through finite element analysis with current design variables. The error vector $\Delta\underline{\theta}$ is the difference between $\underline{\theta}_T$ and $\underline{\theta}_C$.

$$\Delta\underline{\theta} = \underline{\theta}_T - \underline{\theta}_C \quad (4)$$

step3) Obtain the sensitivity matrix from finite difference method. The sensitivity matrix for three frequencies to six design variables is represented as Eq. (5). Elements of the sensitivity matrix are listed on Table 2.

$$Z = \begin{bmatrix} \frac{\partial\theta_1}{\partial\zeta_1}, & \frac{\partial\theta_1}{\partial\zeta_2}, & \cdots, & \frac{\partial\theta_1}{\partial\zeta_6} \\ \frac{\partial\theta_2}{\partial\zeta_1}, & \frac{\partial\theta_2}{\partial\zeta_2}, & \cdots, & \frac{\partial\theta_2}{\partial\zeta_6} \\ \frac{\partial\theta_3}{\partial\zeta_1}, & \frac{\partial\theta_3}{\partial\zeta_2}, & \cdots, & \frac{\partial\theta_3}{\partial\zeta_6} \end{bmatrix} \quad (5)$$

Table 2 Elements of Sensitivity matrix.

	BW	BL	GM	GH	SL	SB
canti-lever	14.7	-46.8	30.7	-59.5	48.5	-42.9
2nd torsion	-3013.6	-1619	1187.1	428	-740	296
sway	-629.4	-1856.0	2595.0	-2363.0	-55.0	-2781.1

The sensitivity equation can be expressed as follows.

$$\underline{\theta}_T = \underline{\theta}_c + Z\Delta\underline{\zeta} \quad (6)$$

step4) Calculate modified values of design variables from Eq. (6). Moreover, the number of target frequencies is greater than design variables and then the right pseudoinverse method is applied as Eq. (7)

$$\Delta\underline{\zeta} = Z^T(ZZ^T)^{-1}\Delta\underline{\theta} \quad (7)$$

step5) Update the design variable vector as like Eq. (8) and then obtain a new current frequency vector $\underline{\theta}_C$ through finite element analysis. Repeat step4 and step5 until $\Delta\underline{\theta}$ is satisfied with a criteria.

$$\underline{\zeta}_{NEW} = \underline{\zeta}_{OLD} + \Delta\underline{\zeta} \quad (8)$$

4.4 Simulation Results

After design variables are obtained, the channel structure is added at the 2nd torsional nodal position to increase the torsional stiffness. The simulation results of mode shapes are shown in Fig. 3.

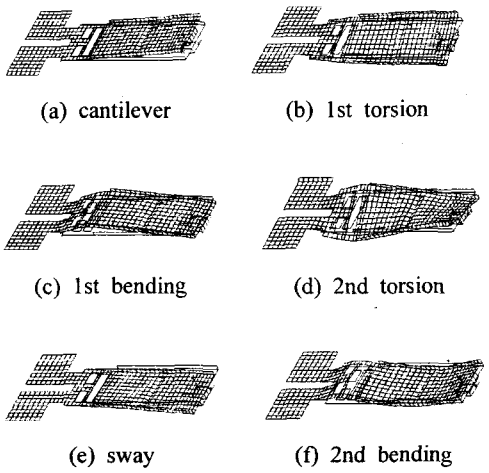

(a) cantilever (b) 1st torsion

(c) 1st bending (d) 2nd torsion

(e) sway (f) 2nd bending

Fig.3 Mode shapes of simulation

5. Experimental Results

Based on the results of the sensitivity analysis, the prototype suspension is fabricated by metal etching process and mechanical forming as shown in Fig. 4, and experiments are carried out in order to identify the dynamic characteristics without air bearing.

Fig.4 Milliactuator embedded suspension

5.1 Modal Analysis and Frequency Response

Experiments for modal analyses and frequency responses are conducted using a Laser Doppler Vibrometer for measurement of the velocity, a dynamic signal analyzer to deal with input-output signals and STAR-MODAL software to estimate modal parameters

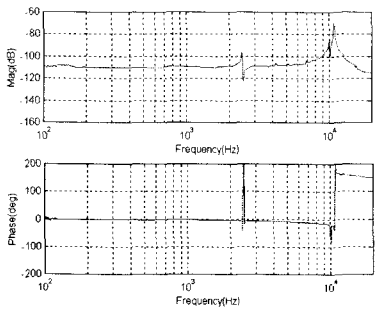

Fig.5 FRF of the suspension with a slider in lateral direction

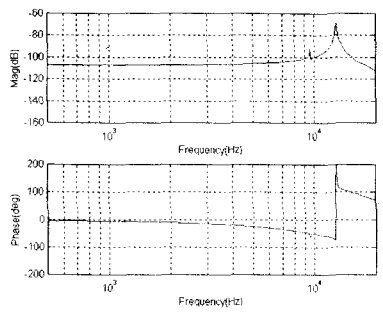

Fig.6 FRF of the suspension without a slider in lateral direction

Fig. 5 and Fig. 6 depict frequency responses of the suspension with and without a slider in lateral direction. The frequency response of the suspension without a slider has two resonance frequencies: the 2nd torsion mode at about 9.6 kHz and sway mode at about 12.8 kHz. The frequency response of the suspension with a slider has the 2nd torsion mode at about 10 kHz and sway mode at 10.8 kHz. Attaching a slider to the suspension makes the resonance frequency of sway mode lowered due to the additional inertial load. In the torsional motion, however, gluing a slider to the suspension has an effect of reinforcing stiffness in the torsional direction and, thus, makes the 2nd torsional mode go up slightly higher. As in Fig. 5, the 1st torsion appears at about 2.4 kHz with a slider. The peak gain of the 1st torsion does not seem to be suppressed sufficiently because the center of mass of the slider is shifted from the rotational axis of the 1st torsional mode by the gluing error of the slider [3]. If the 1st torsion could be depressed with an accurate bonding of the slider or damping material, the suspension's lateral resonance frequency would be at 10 kHz, which is enough to be used for dual-stage actuator systems with 2 kHz bandwidth. Table 3 shows the resonance frequencies of the suspension with a slider in simulation after parameter tuning and experiment. The characteristics of the designed suspension are shown in Table 4.

Table 3 Resonance frequencies of simulation and experiment for the suspension (Hz)

Mode	Simulation	Experiment	Error
Cantilever	245	254	-3.3%
1st Torsion	2515	2440	3.0%
1st Bending	3327	3510	-5.2%
2nd Torsion	10911	10041	8.0%
Sway	11962	10770	10.0%
2nd Ending	15934	15020	5.7%

Table 4 Characteristics of the suspension

Suspension Length (mm)	9	Vertical Spring Constant (N/m)	13.8
Suspension Width (mm)	2.5	Suspension Equivalent Mass (mg)	3.5
Suspension Thickness (mm)	0.05	Head-Disk Separation Acceleration (G/g)	200
Hinge Length	0.1	Hinge Width (mm)	0.75

6. Conclusion

This work has investigated a suspension design scheme with a milliactuator for dual-stage actuator systems. The shear type PZT driving the suspension is selected as milliactuator. The hinge structure carries out two roles, which work as a vertical spring and the milliactuator in the suspension.

The design variables are determined by finite element analysis with the sensitivity analysis. Based on simulation results, the prototype suspension is fabricated and the experiment is carried out to identify dynamic characteristics. The lateral's natural frequency is 10 kHz, which can accomplish higher servo bandwidth for dual-stage actuator systems. The optimized suspension achieves higher mechanical resonance frequencies in the 2nd torsion and the sway mode with a high-shock resistance and a low-spring constant.

Acknowledgement

This research has been supported by KOSEF (Grant No. 2000G0102) and the authors are grateful for the support

References

[1] Ehrlich R. and Curran D., 1999, "Major TMR sources and projected scaling with TPI", IEEE Trans. on Mag., 35, pp. 885-891

[2] Mori K., Munemoto T., Otsuki H., Yamaguchi Y. and Akagi K., 1991, "A Dual-Stage Magnetic Disk Drive Actuator using a Piezoelectric Device for a High Track Density", IEEE Trans. on Mag., 27, pp. 5298-5300

[3] Watanabe T., Ohwe T., Yoneoka S. and Mizoshita Y., 1997, "An Optimization Method Using Pico-CAPS for Precision Positioning", Proceedings of the 1997 IEEE International Conference on Evalutionary Computation, pp. CC-12

[4] Fan L.S., Ottessen H.H., Reiley T.C. and Wood R.W., 1995, "Magnetic Recording Head Positioning at Very High Track Densities Using a Microactuator-Based, Two-Stage Servo System", IEEE Trans. on Ind. Elect., 42, pp. 222-233

[5] Arya S., Lee Y.S., Lu W.M., Staudenmann M. and Hatchett M., 2001, "Piezo-Based Milliactuator on a Partially Etched Suspension", IEEE Trans. on Mag., 37, pp. 934-939

[6] Koganezawa S., Uematsu Y., Yamada T., Nakano H., Inoue J. and Suzuki T., 1998, "Shear Mode Piezoelectric Microactuator for Magnetic Disk Drives", IEEE Trans. on Mag., 34, pp. 1910-1912

[7] Yoon J.H., Yang H.S. and Park Y.P., 2001, "Design and Dynamic Analysis of Suspension for Dual Actuator Type HDD", J. Info. Storage Proc. Syst., 3, pp. 47-51

[8] Ohwe T., Mizoshita Y. and Yoneoka S., 1993, "Development of Integrated Suspension System for a Nanoslider with a MR Head Transducer", IEEE Trans. on Mag., 29, pp. 3924-3926

[9] Tangren J.H., 1998, "Head Suspension for Use with a Dynamic Storage Drive having an Optimized Top Profile Defined by Curved Side Edges", US Patent, 5850319

[10] Adelman H.M. and Haftka R.T., 1986, "sensitivity Analysis of Discrete Structural Systems", AIAA Journal, 24, pp. 823-832

[11] Kajiwara I. and Nagamatsu A., 1993, "Optimum Design of Optical Pick-Up by Elimination of Resonance Peaks", J. Vib. Acous., 115, pp. 377-383